

EXPERIMENTAL STUDY ON THE LONG-TERM PROPERTIES OF PRESTRESSED CONCRETE MEMBERS AFFECTED BY ALKALI-SILICA REACTION (ASR)

Yukio Hiroi^{1*}, Hideki Manabe², Toshiya Ihaya³, Takashi Ookubo⁴, Toyoaki Miyagawa⁵

¹Technical Development Dept., West Japan Branch, PC Bridge Co., Ltd., Japan

²Technical Development Dept., Kansai Japan Branch, Fuji P.S. Corporation, Japan

³Construction Dept., Osaka Branch, Oriental Construction Co., Ltd., Japan

⁴Technical Development, Osaka Branch, Kawada Construction Co., Ltd., Japan

⁵Professor, Department of Civil & Earth Resources, Kyoto University, Japan

Abstract

The purpose of this study is to investigate long-term properties of PC members affected by ASR and to find effective countermeasures. We produced large-scale PC beam specimens modeling an existing structure for the extended monitoring. The specimens have been under outdoor exposure and continuous measurement since its completion in February 2005. The specific focuses of this experiment are residual prestress, long-term deterioration behavior, volume effect of the member and influence of the stirrup rupture.

This paper provides a general plan of the long-term experimental study, an interim report of the outdoor exposure over the past two years and results of a loading test using cracking load.

Keywords: residual prestress, long-term deterioration behavior, volume effect, loading test result

1 INTRODUCTION

Although there had already been several reports of deterioration due to ASR from the Sea of Japan side of the Tohoku and Chugoku regions in Japan before 1970s, this issue had not been recognized as a nationwide problem. Around 1980, some piers were found affected by ASR in the Kinki region, and ASR deterioration was also revealed in structures using concrete containing crushed andesite in the Hokuriku, Chugoku, Shikoku and Kyushu regions. Various standards were established for coping with this issue after that, and four preventive measures were instituted in 1986: proper selection of aggregates; use of low-alkali cements; use of blended cements with preventive effect on ASR; and control over the total alkali content in concrete. This seemed to work successfully for a while. However, the industry was shocked by a case in the Kinki region where stirrups in PC beams were found ruptured in 2003 [1].

Many problems remain to be solved in order to promote control and prevention of ASR deterioration in PC members. Japan Prestressed Concrete Contractors Association established an ASR countermeasure study committee [2] [3] and has been carrying out a long-term exposure test to determine basic performance under ASR deterioration conditions in terms of residual prestress, long-term deterioration behavior, volume effect and shear capacity. The experimental study consists of two series as shown in Figure 1. Experiment series I is designed to determine the basic performance of large-scale PC beams under ASR deterioration conditions, with special focus placed on residual prestress, long-term deterioration behavior and volume effect. Experiment series II is focused on shear capacity to investigate the reduction in shear capacity due to ASR and effect of shear reinforcement. This experimental study has two features: (1) the large-scale specimens modeling an actual structure which were hardly used in previous ASR experiments; and (2) the use of reactive aggregates in the test specimens for comparative examination with control specimens containing normal aggregates.

This paper provides a general plan of experiment series I, an interim report of outdoor exposure over the past two years and results of a loading test at cracking load which was carried out in December 2006.

* Correspondence to: y.hiroi@pc-bridge.co.jp

2 GENERAL PLAN OF THE EXPERIMENTAL STUDY

2.1 Dimensions of the specimens

The following specimens (Table 1) were prepared for experiment series I to determine the deterioration behavior of PC members in actual bridges. This study was also designed to include comparative examination with control specimens containing non-reactive aggregates or with small-scale specimens for assessment. Figure 2 shows the dimensions of the specimens, and Figure 3 shows the concept of evaluations of the specimens.

2.2 Mix proportion of the specimens

The mix proportion for the ASR reactive specimens (containing reactive aggregates) was determined based on mix proportions of the actual structure which exhibited ASR deterioration in a PC beam of a pier. In terms of reactivity, ratios of reactive and non-reactive aggregates were determined by a preparatory test for pessimum proportions (Figure 4). Table 2 shows planned mix proportions for the ASR reactive specimens.

3 MEASUREMENT RESULTS

3.1 Cracking observation

Cracking was observed visually, and image data was recorded using digital cameras. Figure 5 shows cracking observations on the large-scale ASR reactive specimen at the ages of 150 days and 774 days. No remarkable cracks were found on the control specimen (containing non-reactive aggregates), and the ASR reactive specimen exhibited cracks (width: 0.05 to 1.2 mm) along the direction of the prestress or the axis of the member. It is already known that ASR cracking in PC members occurs in the direction of the prestress. Such ASR cracking characteristic to PC members was confirmed in the current experiment.

Figure 6 shows changes in crack density in the large-scale ASR reactive specimen against temperature and precipitation. In general ASR is said to progress more significantly during summertime when temperatures and precipitation are high. This trend was obvious in the current study, with the crack density rapidly increasing during the period from 150 days (July, 2005) to 240 days (October 2005). The increase in crack density then slowed down until 365 days. As the gradients of the curves indicate, the rate of increase again picked up at 614 days with the increases in temperature and precipitation. Density of cracks wider than 0.2 mm was larger in the large-scale specimen than in the small-scale specimen.

Consequently, it was confirmed that the rate of ASR deterioration depended on temperature, precipitation and other ambient conditions, and it also varied depending on the volume of the member.

3.2 Compressive strength and modulus of elasticity

Figures 7 and 8 show compressive strength and modulus of elasticity measured on the cylindrical test pieces which were taken during concrete placement of the specimens. Values of the ASR reactive specimen started to drop clearly at 150 days when cracking became remarkable and showed a drastic drop in modulus of elasticity at 240 days after the first summer. At 774 days, values of the ASR reactive specimen were significantly lower than those of the control specimen: 70% for compressive strength and 20% for modulus of elasticity. However, these values were from the test pieces in which expansion by ASR was not restrained. Expansion in actual structures is restrained by reinforcing bars and others. Therefore, these measurement values may be used as indices only for deterioration in simple concrete but not for deterioration in an actual structure containing reinforcing bars.

3.3 Ultrasonic propagation velocity properties

Figure 9 shows changes in ultrasonic propagation velocity. No remarkable change was found until 90 days in the large- and small-scale specimens. Propagation velocity in the large-scale ASR reactive specimen started to significantly decrease at 150 days, down to about 80% of that of control specimen at 240 days, and continued to decrease then slowly until 774 days. In the small-scale specimen, propagation velocity significantly decreased after 240 days, slowed down as seen in the large-scale specimen, and then reached the same level as the large-scale specimen at 774 days. The difference in how propagation velocity decreased in the large- and small-scale specimens was considered to be due to the volume effect on the rate of ASR deterioration.

3.4 Strain properties

Measurement gauges were installed on the specimens in order to determine long-term strain properties during ASR deterioration (Figure 10). In addition, contact strain gauges were placed at mark intervals of 300 mm on concrete surfaces.

Internal strain in concrete

Figure 11 shows changes in internal strain in concrete at the midsupport of each specimen. Neither specimen showed significant change until measurement on 90 days, suggesting drying shrinkage. In the ASR reactive specimens, a sign of expansion strain was found at 150 days in the large-scale specimen and at 240 days in the small-scale specimen, in the vertical direction and in the direction perpendicular to the bridge axis but not in the prestress direction. The slow expansion continued until 774 days in both specimens. The discrepancy between the large- and small-scale specimens got smaller with age. This tendency is very close to the one seen in the ultrasonic propagation velocity mentioned above.

Prestressing steel strain and tension force

Figure 12 shows changes in prestressing steel strain measured at the midsupport of the large-scale specimen using weld gauges. Figure 13 shows changes in tension force measured using load cells. Although both strain and tension force showed decreases presumably attributable to drying shrinkage and creep, no significant differences were found until 774 days between the ASR and control specimens or between the large- and small-scale specimens. Changes in length in the axial direction of the member measured on concrete surfaces using contact strain gauges were only slight. These measurement results suggest that residual prestress in the ASR reactive specimens is at a similar level to the control specimens at the present time.

Stirrup strain

Figure 14 shows locations of stirrup strain measurement at the midsupport on the large- and small-scale specimens, and Figure 15 shows the measurement results. Stirrup strain showed a sign of expansion after 90 days, and its tendency continued until 774 days. Across the cross section, expansion increase at the top fiber was more significant than at the bottom fiber, suggesting more advanced ASR deterioration on the top side which has been directly exposed to sunlight and rainfall for months.

4 INTERIM LOADING TEST

4.1 Objectives of the test

In anticipation of development of ASR deterioration in the superstructure, loading test was performed on the large-scale specimens in order to examine mechanical behavior during the deterioration. Serviceability limit state load was applied to the specimens, and their properties were determined and verified.

Significant horizontal cracking due to ASR deterioration was found in the specimens after 22 months. Remarkable decrease in modulus of elasticity was observed in the property test using the cylindrical test pieces and also in the ultrasonic measurement. This loading test was designed to check the following points.

- Whether plane sections remain plane properly after horizontal cracking
- Behavior of the actual structure under the decrease in modulus of elasticity
- Restoration performance of the ASR-deteriorated structure

4.2 Experiment plan

The loading experiment used the large-scale ASR and control specimens (I-1-a and I-1-b) for measurement. The test load of 1500 kN was determined to achieve a target stress level in concrete at the midsupport equivalent to bending tensile stress in concrete (-1.99 N/mm^2), without affecting the continued long-term measurement. A hydraulic jack was used for applying the load. Figure 16 shows a view of the loading test.

4.3 Test results

Vertical displacement

As a means to evaluate rigidity of the specimens, vertical displacement was measured using high sensitivity displacement sensors installed at the midsupport and supports. Figure 17 shows the measurement results.

The load-displacement curves suggested that the control and ASR reactive specimens almost retained the linearity. In contrast to the design displacement of 1.42 mm, vertical displacement at the maximum load applied reached 1.53 mm in the control specimens and 1.99 mm in the ASR reactive specimens at maximum, exhibiting a rigidity decrease of about 23% in the ASR reactive specimens. The design values in Figure 17 were calculated from modulus of elasticity of the test pieces containing normal aggregates.

Strain in concrete and reinforcing bars in the direction of the bridge axis

Horizontal cracking which was characteristic to PC structures occurred in the ASR reactive specimens (Figure 5), generating a concern whether originally plane sections in the structure properly remained plane in the vertical direction. For verification of this issue, strain was measured using strain gauges installed on the concrete surface and on the reinforcing bars in concrete placed in the direction of the bridge axis. Figures 18 and 19 show the results at the maximum load applied. As seen in the vertical displacement measurements, the ASR reactive specimen, as compared to the control specimen, exhibited a significant decrease of about 20% in its rigidity. However, no major differences were found in general performance, with no behavior like a "built-up beam" with multiple neutral axes. This proved that plane sections behaved as a whole and remained plane properly in either specimen.

Strain on the concrete surface and that in reinforcing bars in concrete showed similar tendencies, suggesting that the plane sections in the ASR reactive specimen remain plane properly.

5 CONCLUSION

Results of long-term measurement and interim loading test on ASR-affected PC members were reported in this paper. Findings from this study are summarized below.

- (1) Residual prestress in the ASR reactive specimens were equivalent to that in the control specimens after ASR deterioration (degree of deterioration: crack density of 4.8 or above; ultrasonic propagation velocity: about 20% decrease).
- (2) The speed and degree of ASR deterioration varied depending on the volume of a structure.
- (3) Under serviceability limit state loads, ASR-affected specimens were found to maintain plane sections plane properly and retain bond performance of reinforcing bars at levels equivalent to the sound state.

This study shall continue, with a hope that it would help further research into the problem of ASR in PC members.

6 REFERENCES

-
- [1] Japan Society of Civil Engineers (2005): Report of Sub-committee on the countermeasures for the damage due to alkali silica reaction. Concrete Library: I-34.
 - [2] Okubo, T., Manabe, H., Ihaya, T. and Miyagawa, T. (2005): Experimental study on evaluation of long-term properties of ASR-affected prestressed concrete members. Proceedings of the concrete structure scenarios, JSMS, Vol. 5: 179-184.
 - [3] Jodai, K., Manabe, H., Hiroi, Y. and Miyagawa, T. (2006): Report on long-term properties of ASR-affected prestressed concrete members. Proceedings of the concrete structure scenarios, JSMS, Vol. 6: 117-122.

TABLE 1: Specimen types

Specimen No.	Specimen size (mm)	Aggregate type	Specimen name
I-1-a	Large-scale (1200 x 1250 x 7500)	Reactive	Large-scale ASR reactive specimen
I-1-b		Non-reactive	Large-scale control specimen
I-2-a	Small-scale (535 x 560 x 4000)	Reactive	Small-scale ASR reactive specimen
I-2-b		Non-reactive	Small-scale control specimen

TABLE 2: Mix proportions for the ASR reactive specimens

Air: Air content (%); W/C: Water/cement ratio (%); W: Water; C: Cement; A: Admixture

* Ratios are to be determined by the test for pessimum proportions.

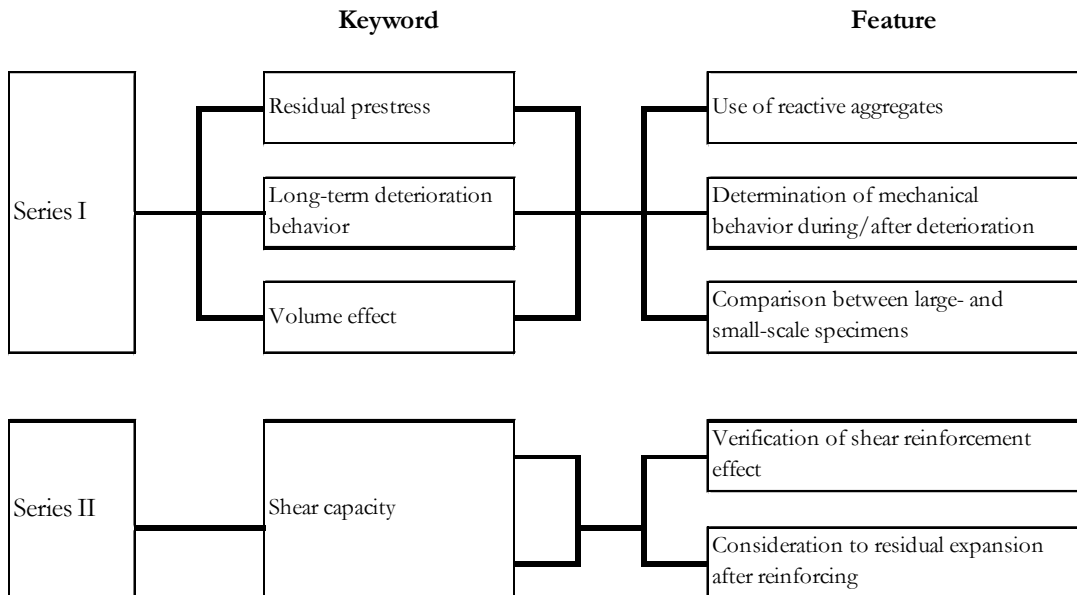


Figure 1: Schematic view of the experiment

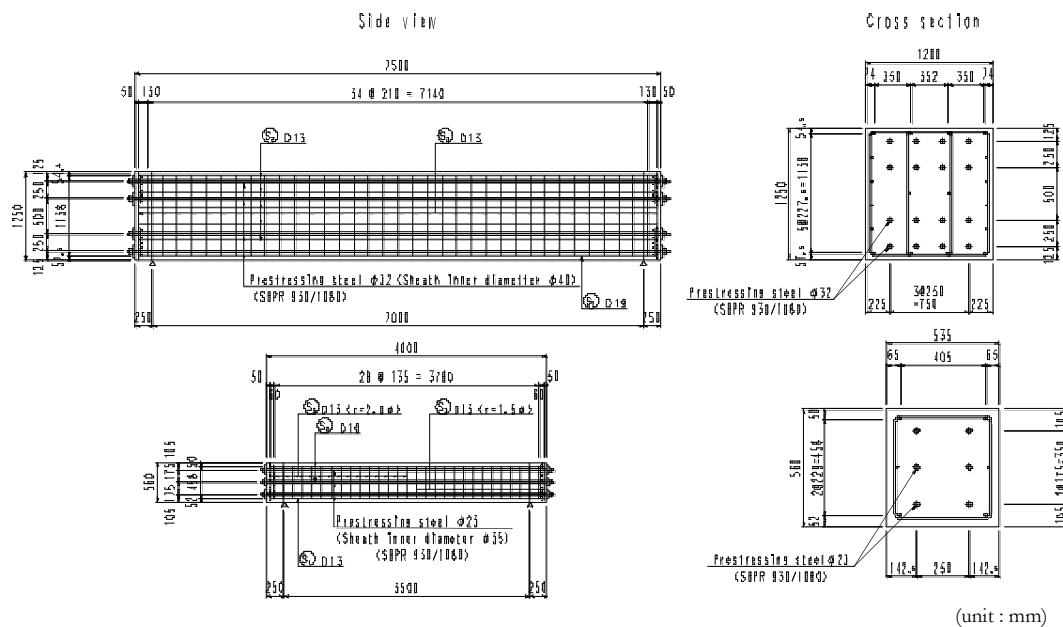


Figure 2: Large- and small-scale specimen dimensions

$A = (I-1-b)/(I-1-a)$: Degree of ASR deterioration
$B = (I-2-b)/(I-2-a)$: Degree of ASR deterioration
$C = A/B$: Volume effect on ASR deterioration

Figure 3: Conceptual view of specimen evaluation

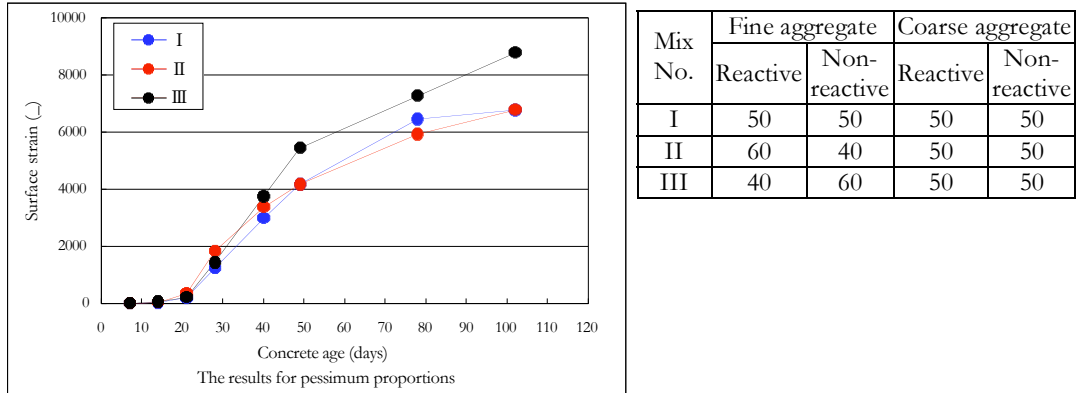


Figure 4: Test results for pessimum proportions

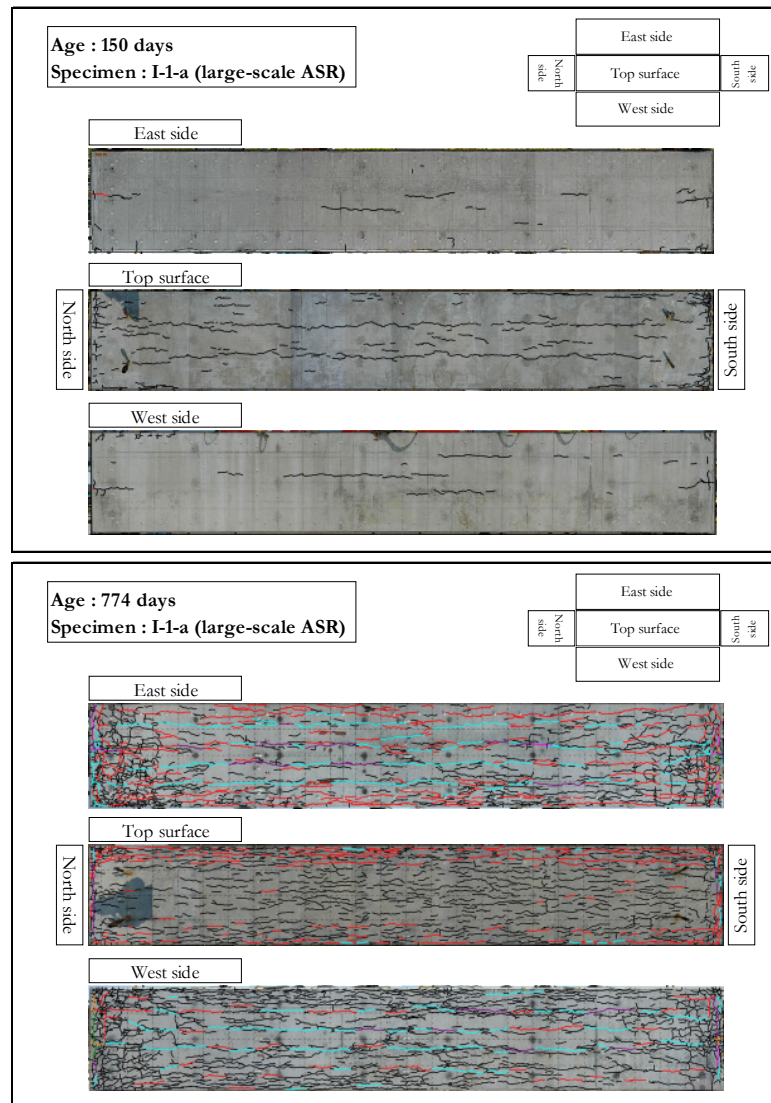


Figure 5: Cracking on the large-scale ASR reactive specimen

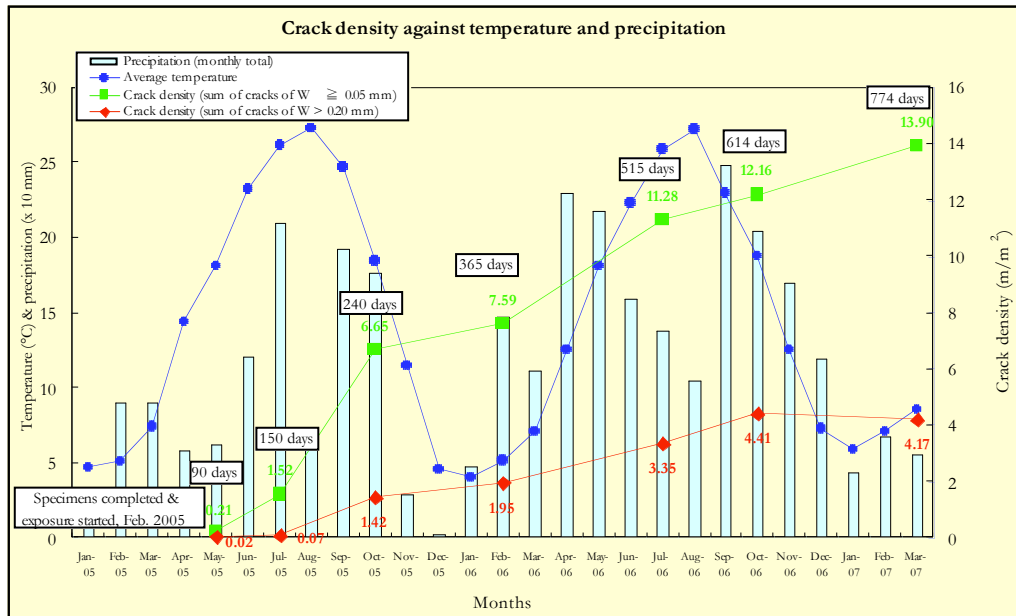


Figure 6: Crack density against temperature and precipitation

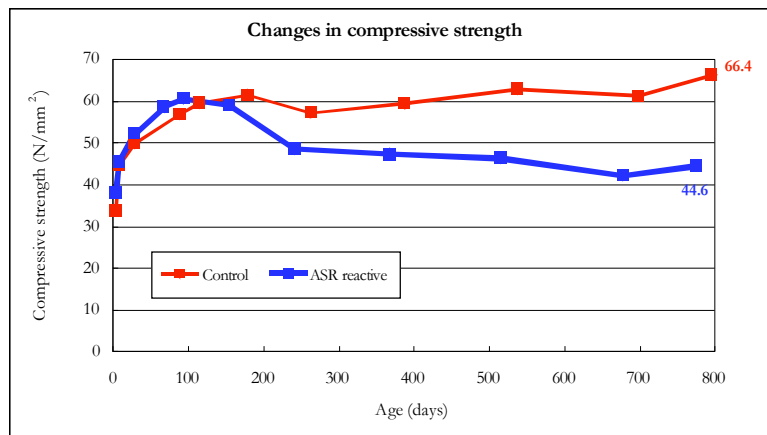


Figure 7: Changes in compressive strength

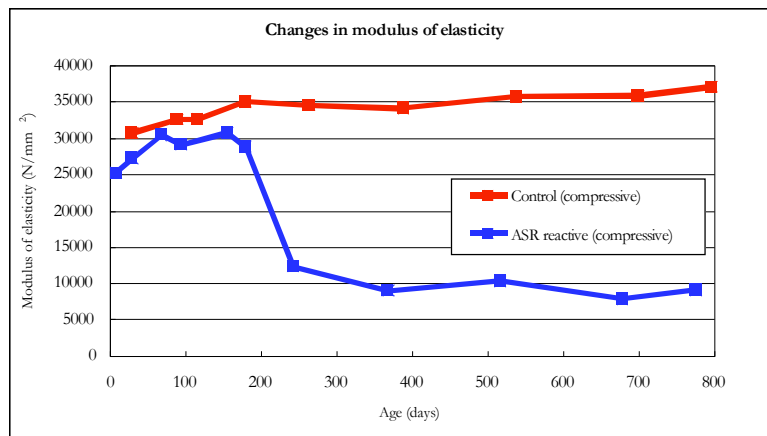


Figure 8: Changes in modulus of elasticity

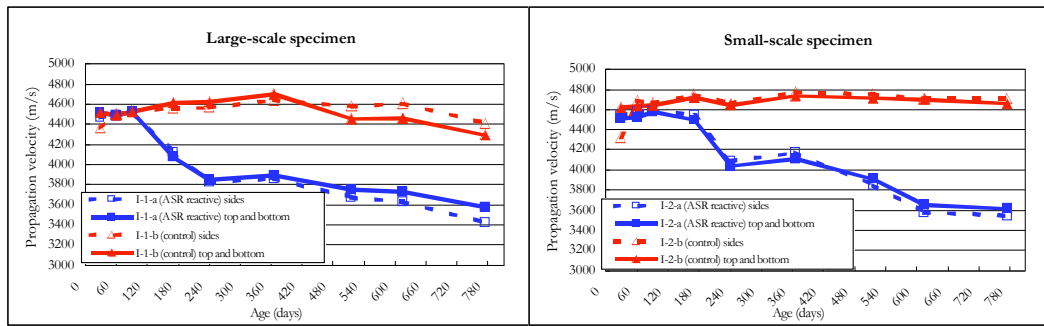


Figure 9: Changes in ultrasonic propagation velocity -- large- and small-scale specimens

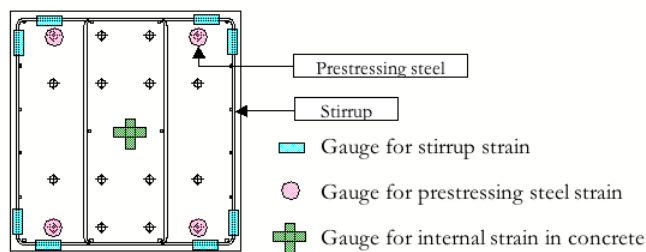


Figure 10: Locations of the measurement devices

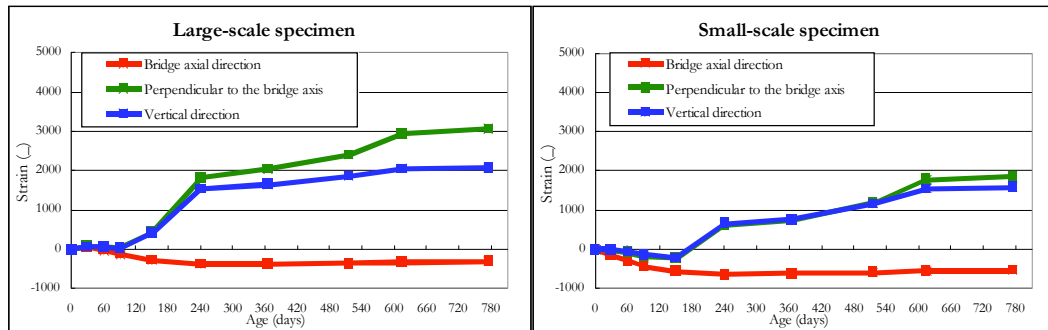


Figure 11: Changes in internal strain in concrete

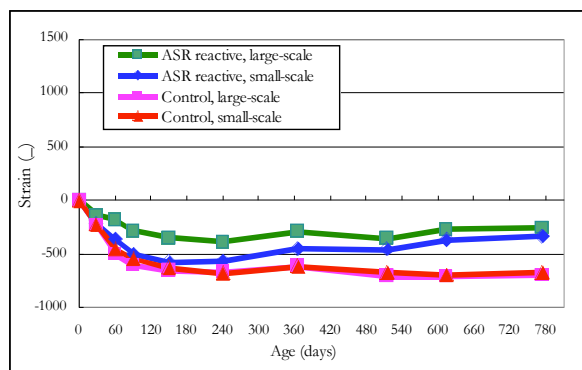


Figure 12: Changes in prestressing steel strain

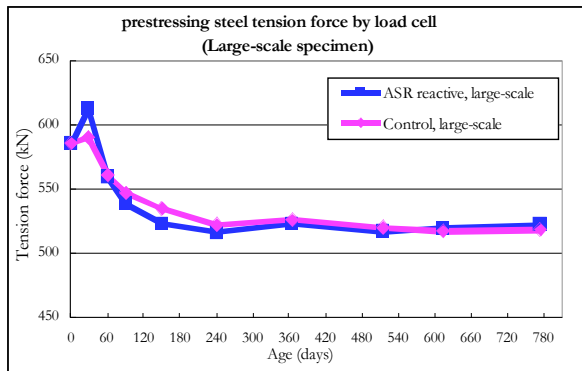


Figure 13: Changes in prestressing steel tension force

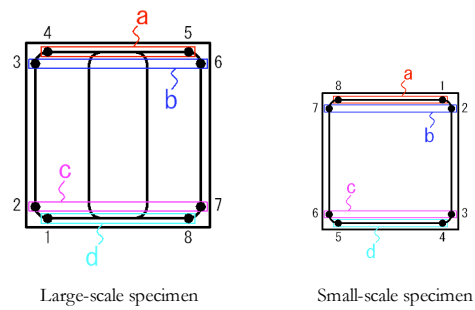


Figure 14: Stirrup measurement locations

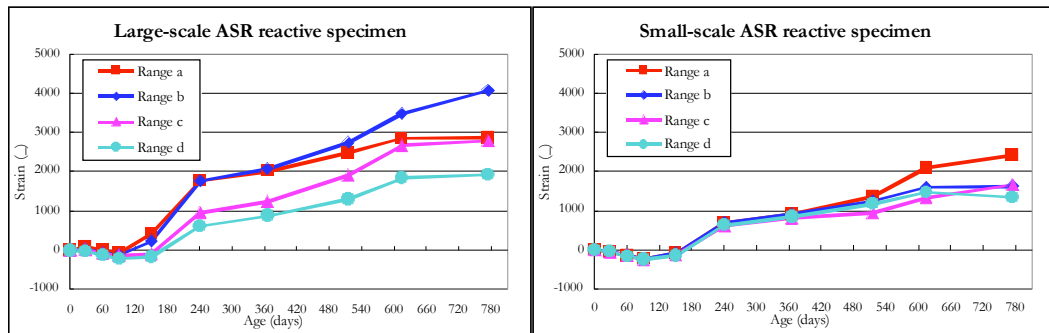


Figure 15: Changes in stirrup strain



Figure 16: Loading test

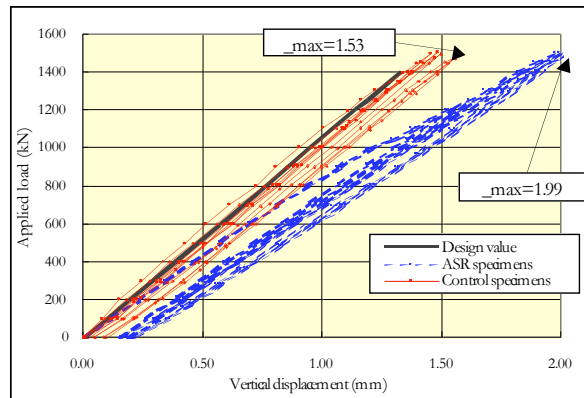


Figure 17: Load-displacement relationship

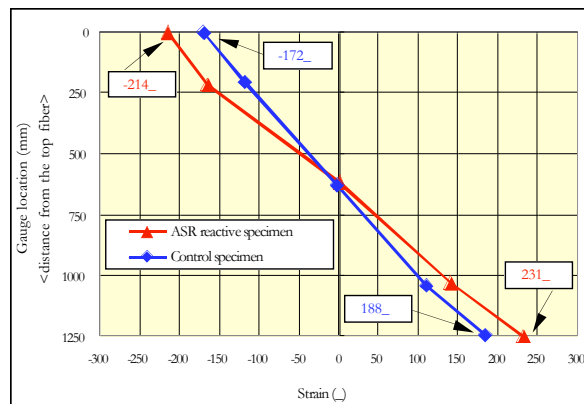


Figure 18: Concrete surface strain

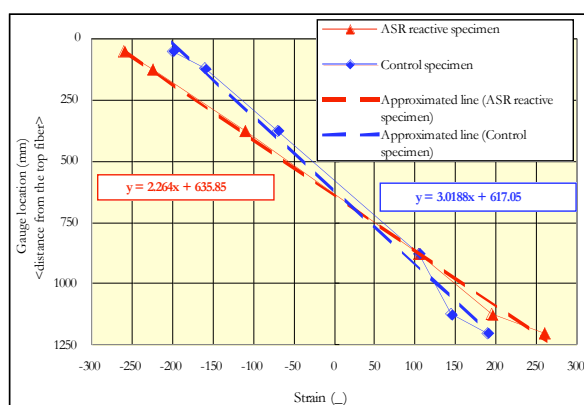


Figure 19: Approximate equation of internal strain

